CONTRIBUTIONS

INTERPLANETARY

Flare Induced Shocks and Corotating Streams in the Interplanetary Medium

M. WISEMAN AND P. A. DENNISON
Department of Physics, University of Adelaide

Geomagnetic storm sudden commencements (ssc) and sudden increases (si) can be caused by either a propagating discontinuity (i.e. a hydromagnetic shock or blast wave) in the interplanetary plasma or by the convection past the Earth of a discontinuity in the ambient solar plasma flow.

A flare produced disturbance tends to propagate through the interplanetary medium as a plasma wave preceded at its leading edge by a supersonic shock. Akasofu and Yoshida[1, 2] have inferred a three dimensional structure for the solar plasma flow generated by solar flares. The disturbance consists of a narrow jet of plasma which contains the energy for the main phase of the geomagnetic storm, and a roughly hemispherical shock wave which initiates the sudden commencement.

Hirshberg[3] has shown that the shape of the shock front departs considerably from Sun-centred radial symmetry and that it tends to advance on a much broader front. Ballif and Jones,[4, 5] however, have argued that individual flares are not the cause of either Forbush decreases or geomagnetic storms, but that these phenomena can be accounted for entirely by corotating interplanetary streams. This view is in contrast to the work of Burlaga and Ogilvie[6] who examined magnetic field and plasma data for 19 geomagnetic events and showed that out of these, 12 were caused by hydromagnetic shocks and 7 by tangential discontinuities in the density of the solar wind.

Unfortunately, since space probes are at present confined to the ecliptic plane, there is a limit to the amount of information which can be gained about the overall structure of such disturbances to resolve this problem.

In a previous paper[7] we have discussed a method for mapping the movement and geometry of large scale features of the solar wind by observation of the interplanetary scintillation (IPS) of a grid of discrete radio sources. Using this method, the origin and development of both types of disturbance which we have discussed, have been observed and recorded during June 1969. We show that both plasma blast waves and corotating streams can be primary agents in the onset of geomagnetic storms, and that IPS is a powerful method for investigating the structure of such phenomena.

OBSERVATIONS

The work was carried out from May 31 to June 26, 1969 using the CSIRO 80 MHz Radioheliograph at Culgoora, N.S.W. The observing procedure and subsequent analysis is essentially the same as that described in a previous paper.[7] A 'grid' of radio sources, spaced as evenly as possible about the celestial sphere, were observed every day, and a representative sample of their scintillation was recorded on magnetic tape for later computer analysis. We have assumed that the dominant scattering region for a particular source is normally located around the point of closest approach to the Sun by the line-of-sight to the source.

RESULTS AND DISCUSSION

Two major regions of activity dominated the solar disc during June 1969. Region A, which had central meridian passage (CMP) day on June 10 was extremely flare-active with large associated radio flux at 21 cm, 43 cm and particularly at 10.7 cm, where the flux exceeded ten times the estimated quiet Sun level. The region was prominently flare active for four solar rotations prior to June. (Solar data are from the Solar Geophysical Data Bulletins, Department of Commerce, U.S.A.)

Region B (CMP June 19) was a relatively short lived region, which was extremely flare-active during May but subsided to moderate activity in the space of one solar rotation. The associated radio flux was large at 10.7 cm, and also at 21 and 43 cm. The region faded and lost its identity during the following rotation.

The activity of region A was dominated on June 5 by several very strong flares at N10° E60° from 1000-1700 U.T. Two flares of class 3B were recorded with duration between one and two hours, accompanied by two class 2B and several smaller flares of duration 10 minutes to 2 hours. In Figure 1 the scintillation indices for fourteen sources over the 27 day period of observation are shown. The most significant feature of this figure is the large increase in scintillation shown by most sources between June 6-8.

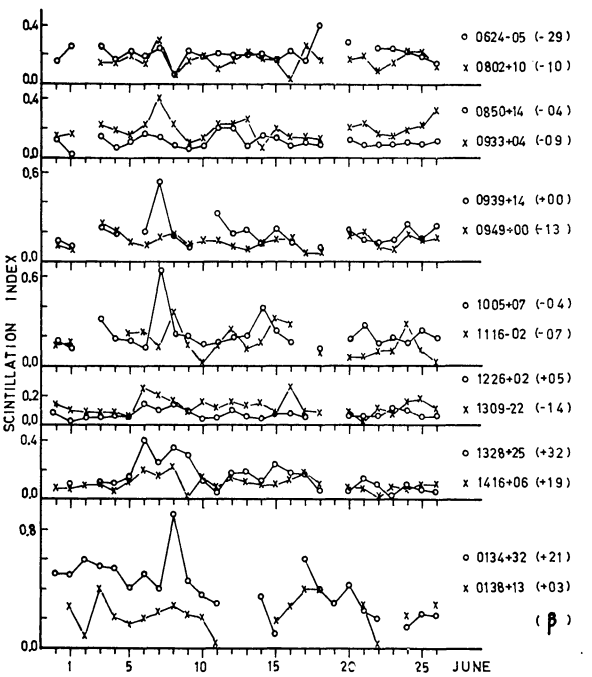

Figure 1. The scintillation indices of 14 sources observed during June, 1969.

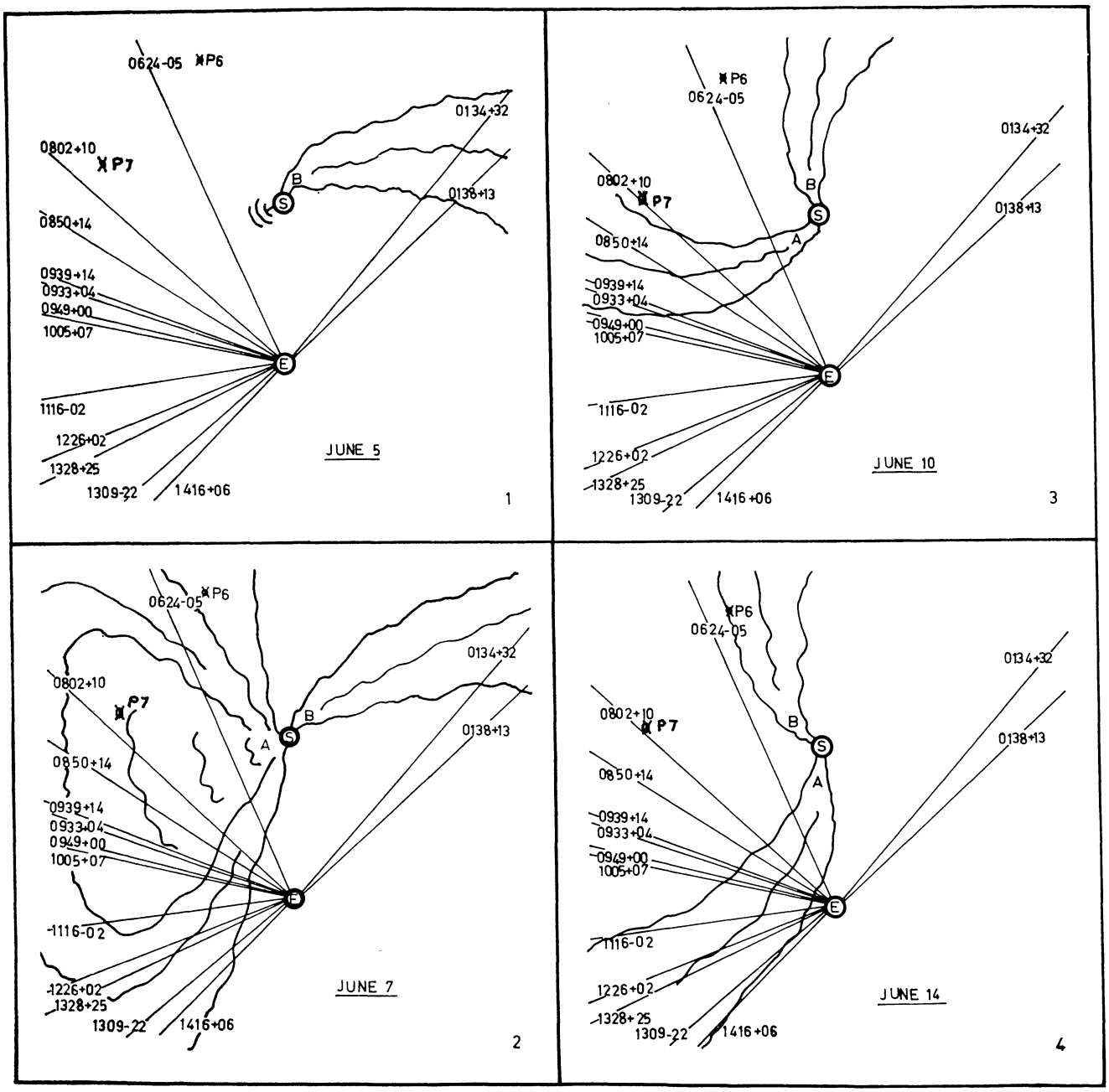

Figure 2. Sketches showing the proposed large-scale structures in the interplanetary medium during June 1969.

Sources 0933 + 04, 1005 + 07, 1309 − 22 and 1328 + 25 showed a 300% increase in scintillation index, while sources 0802 + 10, 0850 + 14, 0949 + 00, 1226 + 02 and 1416 + 06 showed more moderate increases. The absence of a major time sequence in the changes of the indices suggests that the increases were produced by a radial blast of turbulent plasma moving out from the Sun. The observations exclude the alternative possibility of a corotating structure in the solar wind, which would have required about 5 days to move from source 0802 + 10 to source 1416 + 06. The fact that flare region A on the Sun's eastern limb was extremely active only a short time before, strongly suggests a causal connection between the blast and the flare region. The shape of the index curves over a number of sources at different ecliptic latitudes provides evidence of a non-istropic blast structure perpendicular to the ecliptic plane. The ecliptic latitude (β) of each source is listed beside the appropriate index plot in Figure 1. Sources lying close to, or south of the ecliptic plane (0802 + 10, 0939 + 14, 1005 + 07, 1116 − 02) showed a sharp one day increase on June 7 and 8, while sources well north of the ecliptic showed increases of several days duration. 1416 + 06, which is 19° north of the ecliptic, exhibited an increase over 3 days and 1328 + 25 ($\beta = 32°$) showed a width of 3-4 days. This would appear to indicate that the origin of the blast was in the northern

solar hemisphere, which fits in well with its proposed origin in region A at 10°N. The arrival of the blast at the Earth on June 8 caused a 200% increase in the index of 0134 + 32, and Earth satellites Vela 3 and 4 recorded a sudden velocity increase from 250-450 km/sec at 0700 U.T. on the same day. A sudden commencement geomagnetic storm, also on June 8, was accompanied by a 3% Forbush decrease recorded at the Deep River neutron monitor.

An important feature of the blast wave was its velocity profile in the ecliptic plane. The spacecraft Pioneer 7 recorded a velocity increase from 500 to 650 km/sec on June 7, which contrasts with the much lower velocity measured by the Vela satellites. Positions of the Pioneer spacecraft are shown in Figure 2. The velocity anisotropy of the blast could have been either inherent in the original blast structure or caused by the interaction of the blast with the ambient interplanetary plasma and magnetic field. If we assume that the flare activity in region A between 1000-1700 U.T. on June 5 was the source of the blast, then the measured propagation speed at the Earth (450 km/sec) was lower than the calculated mean transit velocity (600 km/sec), which implies a deceleration of the blast after its formation at the Sun. This problem has been treated by Hundhausen and Gentry[9] and by De Young and Hundhausen,[10] using numerical methods to simulate the observed conditions associated with such blasts. The symmetry axis of the initial blast on June 5 was 35° from the Sun-Pioneer 7 line and 60° from the Sun-Earth line, with transit times over these paths of 55 and 70 hours respectively. From the theoretical[10] shock shapes at 30° and 60° to the symmetry axis we can estimate the transit time of the blast to 1 A.U. along the symmetry axis. This was of the order of 45 hours, and is equivalent[10] to an initial blast disturbance energy of $\sim 10^{31}$ ergs.

Following the effects of the blast there was evidence that a continuing flux of plasma gave rise to a stream which corotated with the Sun during the rest of the month, causing sequential increases in the scintillation indices over the grid of observed sources. The time at which the stream met the Earth was estimated from its effect on sources 1309—22, 1328 + 25 and 1416 + 06, since their lines of sight shown in Figure 2 are closest to the Sun at the point at which they intercept the Earth. Sources 1309 — 22 and 1416 + 06 were affected on June 16 and 17 respectively, while 1328 + 25, which is 32°N of the ecliptic plane was affected on June 15. A sudden commencement geomagnetic storm on June 16 accompanied the arrival of the stream at the Earth. By June 17 the Earth was embedded in the stream, and the lines of sight to 0134 + 32 and 0138 + 13 intercepted the leading edge of the stream, causing a 200% increase in their scintillation indices.

We now turn to the remaining sources to examine their agreement with our corotating stream model. Sources 0850 + 14, 0933 + 04 and 0939 + 14 showed enhanced scintillation on June 11, followed by 1005 + 07 on June 14, 1116 — 02 on June 15 and 1309 — 22 on June 16. Figure 2 shows the estimated position of the stream and blast wave during this period.

An estimate of the width of the stream in the ecliptic may be made from the shape of the index plots. Sources, which were south of or in the ecliptic exhibited widths of the order of one day, whereas 1328 + 25 and 1416 + 06, which were both more than 19° north of the ecliptic, showed widths of between two and four days. Thus in the vicinity of the Earth the stream had an approximate width of 0.6 A.U. north of the ecliptic tapering to approximately 0.2 A.U. below the ecliptic.

The second region of interest on the solar disc during June was the flare group at latitude 8° North having CMP date June 19. There was evidence of an associated weak plasma stream from this region corotating with the Sun over the period of observation.

The Earth satellites Vela 3 and 4 recorded an increase in the solar wind velocity from 300-450 km/sec on May 29-30, apparently associated with a 2-3% Forbush decrease on May 28 and 29. The continuing effect of the stream may be seen in the enhanced scintillation index of 0134 + 32 from June 2-4, and of 0138 + 13 on June 3. The fact that 0134 + 32 ($\beta = 32°$) showed enhancement over two days compared with only one day for 0138 + 13 ($\beta = 3°$) is an indication of the stream's geometry perpendicular to the ecliptic plane. The general enhancement in the index of 0134 + 32 until June 7 is interpreted as the effect of the line of sight to the source passing through an extended region of the stream as it receded from the Earth.

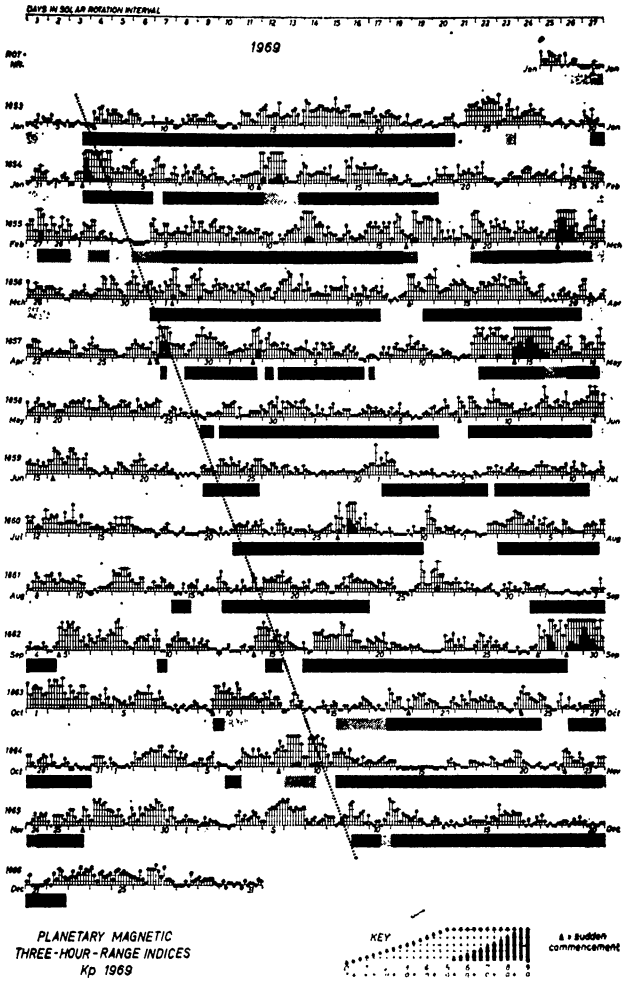

Figure 3. The magnetic field sector structure during 1969 (after Wilcox & Colburn (1971)), superimposed on a plot of K_p indices. Heavy shading denotes field towards the sun, and light shading away from the sun. Positions I, II and III correspond to the plasma blast and streams A and B described in the text.

Half a solar rotation later, on June 18, 0624 — 05 exhibited a 200% increase in its index. This increase was then observed to move sequentially through the sources whose lines of sight lay to the east of the Sun; 0802 + 10 on June 17, 0933 + 04 and 1005 + 07 on June 21, 1226 + 02 on June 23 and 1309 — 22 and 1328 + 25 on June 24-25. The relatively small changes in scintillation index on these sources emphasizes the weakness of the disturbance, and consequently no geophysical events were apparent when the stream met the Earth again.

CONCLUSIONS

A recent paper by Wilcox and Colburn[11] presenting the positions of the quiet Sun magnetic field sector boundaries for 1969 lends strong support to the interpretation of our scintillation results. Figure 3 is a reproduction of the sector boundary crossings during 1969. A reversal of the dominant field polarity from June 7-8 coincided exactly with the position of the blast wave which we have deduced from scintillation observations. The width of the field reversal at the Earth (1 day) also agrees well with our estimate of the width of the blast in the ecliptic plane. When the associated plasma stream corotated past the Earth on June 15-16, it was preceded by a reversal in the polarity of the solar magnetic field on June 14. Thus the stream which we have analysed corresponded to the turbulent region of plasma which is known to accompany magnetic field sector boundaries. Both of the abovementioned events were associated with sudden-commencement geomagnetic storms on June 8 and June 16.

The weaker stream from region B on the Sun can be seen (Figure 3) to be associated with a sector boundary crossing on June 23 when the dominant field polarity was again reversed.

Thus it is evident that the IPS of a grid of radio sources is a particularly useful method for tracing the development of interplanetary streams, plasma blasts and magnetic field sector boundaries in the solar wind. We have shown that both streams and plasma blasts are primary agents in the onset of sudden commencement geomagnetic storms, and that corotating streams are often associated with the sector boundaries in the solar magnetic field.

It is a pleasure to thank Dr J. P. Wild and the staff of CSIRO for making the radioheliograph available for the observations. One of us (M.W.) acknowledges the support of a Commonwealth Postgraduate Award.

Note in proof: Consideration of the power spectra of the scintillations has revealed a more detailed structure of the streams which will be described in a later paper.

[1] Akasofu, S. I. and Yoshida, S., *Planet. Space Sci.*, **15**, 39 (1967).
[2] Akasofu, S. I. and Yoshida, S., *Planet. Space Sci.*, **15**, 942 (1967).
[3] Hirshberg, J., *Planet. Space Sci.*, **16**, 309 (1968).
[4] Ballif, J. R. and Jones, D. E., *J. Geophys. Res.*, **74**, 3499 (1969).
[5] Ballif, J. R. and Jones, D. E., *J. Geophys. Res.*, **74**, 3512 (1969).
[6] Burlaga, L. F. and Ogilvie, K. W., *J. Geophys. Res.*, **74**, 2815 (1969).
[7] Dennison, P. A. and Wiseman, M., *Proc. ASA*, **1**, 142 (1968).
[8] Wild, J. P. (ed.), *Proc. IREE Aust.*, **28**, No. 9 (1967).
[9] Hundhausen, A. J. and Gentry, R. A., *J. Geophys. Res.*, **74**, 2908 (1969).
[10] De Young, D. S. and Hundhausen, A. J., *J. Geophys. Res.*, **76**, 2245 (1971).
[11] Wilcox, J. M. and Colburn, D. S., *Nature Phys. Sci.*, **233**, 48 (1971).

Bessellian Spectral Analysis of Interplanetary Scintillation

B. D. Ward, R. G. Blesing and P. A. Dennison
Department of Physics, University of Adelaide

It is now well established that observations of interplanetary scintillation from a single station can yield useful information on the angular structure of radio sources,[1] and on the propagation of large-scale disturbances through the interplanetary medium.[2, 3] However, when it is required to obtain detailed information on the plasma properties single station observations suffer from the disadvantage that, in general, it is not possible to measure the velocity and scale of the irregularities independently. For example, a change in the width of the observed temporal power spectrum of the scintillations might be caused by either a change in velocity, or a change in scale, or a combination of both.

Lovelace *et al.*,[4] recently pointed out that under certain conditions the observed power spectrum might develop a modulation from which the velocity of the drifting diffraction pattern (and hence the solar wind) could be determined. More recently[5] the technique has been applied to ionospheric scintillations and to some interplanetary scintillation data.

It is the purpose of this paper to examine the dependence of the modulation on various solar wind parameters, in particular the distance of the scattering region from the observer, the thickness of the scattering layer, and the presence of other than a single well-defined velocity. In addition we discuss some observations of scintillation at 80 MHz which we have analysed using these techniques.

For the case of a thin, weakly scattering layer (rms phase deviation $\phi_0 < 1$), the two dimensional intensity power spectrum at a distance Z from the layer can be approximated by,[6]

$$P_I(q_x, q_y) = P_\phi(q_x, q_y) \sin^2\left(\frac{\lambda Z}{4\pi} q^2\right), \qquad (1)$$

where q_x and q_y are spatial frequencies, $q^2 = q_x^2 + q_y^2$, and P_ϕ is the power spectrum of the phase fluctuations imposed on emergence from the layer. The spectrum is modulated by the $\sin^2$ term and in this ideal case the modulation minima extend to zero. By applying a two-dimensional Fourier transform to the two-dimensional autocorrelation function, $\rho_I(r_x, r_y)$, of the diffraction pattern on the ground, $P_I(q_x, q_y)$ could be found. However, a single station can yield only a cross-section, $\rho_I(r_x, 0)$, of the autocorrelation function. Normal procedure is to obtain the power spectrum from this observed function via a one-dimensional Fourier transform, but in so doing the modulation is smeared since this function is actually the projection of the two-dimensional power spectrum onto one-dimension. If circular symmetry is assumed (which corresponds to isotropic scattering irregularities), the Bessel transform of $\rho_I(r_x, 0)$ may be formed to yield the two-dimensional Fourier transform,

$$P_I(q) = \int_0^\infty \rho_I(r)\, r J_0(2\pi q r)\, dr,$$

where $r^2 = r_x^2 + r_y^2$. Thus the modulation is retained,

and it is in principle possible to determine the velocity from the positions of the zeros which in equation (1) occur when

$$\frac{\lambda Z}{4\pi} q^2 = n\pi\,, \qquad (n = 0, 1, 2, \ldots..)\,.$$

For a single, well-defined velocity u, the temporal frequencies at which the dips occur are then given by,

$$= \frac{\sqrt{n}\, u}{\sqrt{\lambda Z}}\,. \qquad (2)$$

So far we have assumed a thin scattering screen. Salpeter[7] derived an expression for the two-dimensional power spectrum arising from an extended scattering region of thickness L,

$$P_I(q_x, q_y) = P_\phi(q_x, q_y) \left[1 - \frac{4\pi}{L\lambda q^2} \sin\left(\frac{L\lambda}{4\pi} q^2\right) \cos\left(\frac{2Z\lambda}{4\pi} q^2\right)\right],$$

from which it is clear that for an extended layer the minima no longer reach zero. In most cases we expect this extended screen to be a more realistic model than the thin screen. To illustrate the effect of varying the distance Z and thickness L of the screen, spectra at 80 MHz have been computed and are shown in Figure 1. As the screen is approached the minima move to higher frequencies and therefore become more difficult to observe. As the thickness of the screen is increased the minima become smeared as expected from the expression for $P_I(q_x, q_y)$. The assumed form of the phase function P_ϕ affects the slope of the power spectrum but not the position of the minima. It can be seen from Figure 1 that the reduced slope of the spectrum computed using a power-law phase function allows minima to be observed out to higher frequencies than for the case of a Gaussian phase function. In both cases an irregularity scale of 200 km was used.

In addition to the above effects, further smearing of the modulation pattern is expected due to the variation of the

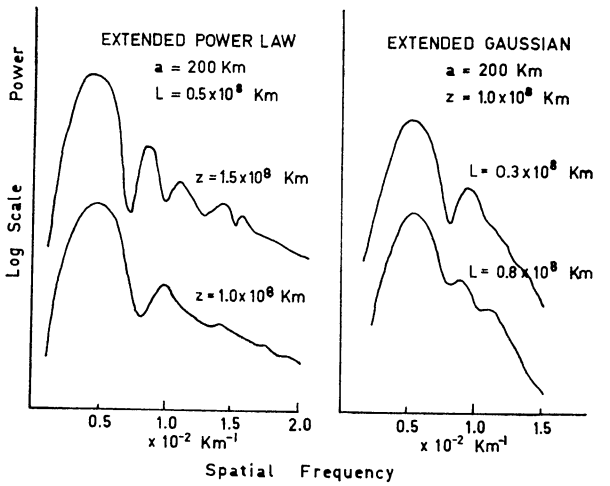

Figure 1. Computed power spectra showing the effects of varying the distance Z or the thickness L of the scattering layer.

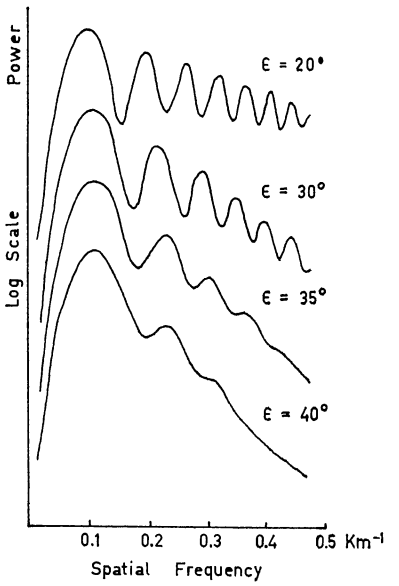

Figure 2. The effects of integration along an extended line of sight, for various elongations ϵ of the source relative to the Sun. The spectra were computed for an observing wavelength of 1 cm.

projected velocity of the plasma at different points along the line-of-sight. To assess this purely geometrical effect, power spectra have been computed for several elongations by dividing the medium into a series of thin screens along the line-of-sight, and adding the contributions from each with a weighting factor proportional to the scattering power of the medium (r^{-4}, where r is the distance from the Sun). A Gaussian phase spectrum was used with a width dependent on the scale of the irregularities, a. Values for the scale were taken from Readhead,[8] and vary from 20 km at $r = 0.1$ A.U. to 220 km at $r = 1$ A.U. The results are shown in Figure 2, from which it is apparent that the modulation is blurred rapidly for elongations $\gtrsim 35°$. This rapid onset of blurring is the result of both the geometrical velocity effect and also the increase in scale, a, which steepens the spectra. It is also clear from Figure 2 that as the geometrical effect increases at larger elongations, the reduction of the apparent ('integrated') velocity causes the minima to move to higher spatial frequencies. The spatial frequencies indicated on the axis of Figure 2 correspond to an observing wavelength of 1 cm.

Apart from the above-mentioned geometrical effect, a range of velocities might exist even at a fixed distance Z. The effect of such a random velocity field is shown in Figure 3, where the spectrum was computed for a thin screen at a fixed distance, with the velocity varying $\pm$ 25 km/s about its mean value, and for an observing frequency of 80 MHz.

Over the past three years the Adelaide radio astronomy group has amassed a considerable amount of scintillation data from observations at 80 MHz using the CSIRO Radioheliograph at Culgoora, N.S.W. Consideration of the above results, however, indicates that at this frequency under ideal conditions, only two or three minima might be expected in our spectra (normally derived from $\sim$ 10 min of observation) before the power decreases to that of the noise spectrum. Integration along an extended line of sight and the possible presence of velocity dispersion[9] add